APPLICATION OF THE THERMODYNAMICAL MODEL TO πN AND KN COLLISIONS, AND CHARGED AND NEUTRAL STRANGE PARTICLE PRODUCTION

By K. Hänßgen

Sektion Physik, Karl-Marx-Universität, Leipzig*

(Received April 2, 1976)

In the present paper we reformulate the thermodynamical model and compare the model calculations of invariant inclusive single particle distributions with experimental data. We apply the model to hadron-hadron collisions especially to Kp, πp and pp reactions and consider the production of neutral, strange and charged particles; carefully respecting kinematical limits and quantum number conservation. The calculated spectra are in agreement with the data of differential and integrated invariant inclusive single particle cross sections.

1. Introduction

The thermodynamical model has been used successfully in calculating inclusive single particle spectra [1–6]. Particle production in the thermodynamical model proceeds in two steps:

(*i*) fireball production via multiperipheral or uncorrelated mechanisms;

(*ii*) fireball decay.

Fireball production functions were considered in Refs [4, 7, 8]. The mechanisms of fireball decay were investigated in great detail using the statistical bootstrap model [9, 10]. A phase space cut-off near the kinematical limits was introduced [11]. The average central fireball mass was determined to be about 1.5 GeV with the help of two particle correlations [12].

The aim of this paper is the reformulation of the model to describe collisions of any pair of hadrons such as pp, πp, Kp etc. taking into account the progress mentioned above during the last years. The effects resulting from kinematics and quantum number conservation are treated carefully.

We compare the model with the production data for p, $K^{\pm}$, $\pi^{\pm}$, $\Sigma^{\pm}$ and neutral particles such as Λ, $\bar{\Lambda}$, K^0, $\overline{K^0}$ in Kp, pp and collisions.

In Section 2 we describe our model for calculating the spectra. In Section 3 we compare the calculated distributions with experimental data and discuss the results.

* Address: Sektion Physik, Karl-Marx-Universität, 701 Leipzig, Karl-Marx-Platz, DDR.

2. Single particle spectra according to the thermodynamical model for collisions of hadrons h_1 and h_2

We calculate the spectra due to contributions (see Fig. 1) of newly produced and through-going particles as well as particles produced via resonances with and without quantum-number exchange. The model which was mostly applied to proton collisions

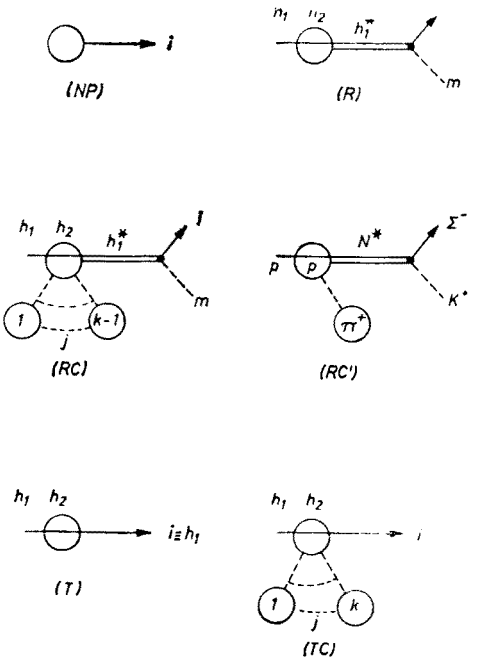

Fig. 1. Graphical representation of the contributions of the thermodynamical single particle spectra of particle i in hadron (h_1-h_2) collisions: (NP) — newly produced particles, (R) — production via leading resonances ($h_{1,2}^*$), (RC) — production via leading resonances with quantum number exchange and additionally produced particles $1 \leqslant j \leqslant k-1$, (T) — through-going particles, (TC) — through-going particles with quantum number exchange and additionally produced particles $1 \leqslant j \leqslant k$, (RC') — special example for (RC): $pp \to N^* \to \Sigma^-(+K^+)$, π^+ is the additionally produced particle

(see [1, 3–5]) is extended to collisions of hadrons of a different kind, i.e. h_1 and h_2. Considering newly produced particles, we discuss in detail the modifications of the thermodynamical expressions necessary for h_1-h_2-collisions. The other contributions to the spectra are discussed in less detail.

(*i*) Newly produced particles (NP, Fig. 1)

In pp collisions this term is calculated according to (see [3, 8])

$$E\frac{d^3N_{\mathrm{NP}i}}{d^3p} = \int G(\eta, \sqrt{s})\mu_i \cosh(\eta_i-\eta) g_i(\eta, \sqrt{s}) f_i\left(\frac{\mu_i \cosh(\eta_i-\eta)}{T(M_{\mathrm{F}}, \sqrt{s})}\right) d\eta \tag{1}$$

with

$$g_i(\eta, \sqrt{s}) = G_i \exp\left(-\frac{m_i}{T(M'_{\mathrm{F}})} + \frac{m_i}{T(M_{\mathrm{F}})}\right). \tag{1a}$$

The kinematical allowed region $1-\eta_t \leqslant \eta \leqslant 2\eta_p$ of particle production changes for collisions of two different hadrons h_1 and h_2, because the fireball rapidity range attains other limits. We denote the primary particles as target (t) and projectile (p). From energy--momentum conservation we get in the centre of momentum system (CMS) the rapidity limits:

$$\eta_{p,t} = \cosh^{-1}(\gamma_{0_{p,t}}), \tag{2}$$

$$\gamma_{0_p} = \frac{s+m_p^2-m_t^2}{2\sqrt{s}\,m_t} \text{ forward direction,} \tag{2a}$$

$$\gamma_{0_t} = \frac{s+m_t^2-m_p^2}{2\sqrt{s}\,m_t} \text{ backward direction.} \tag{2b}$$

We consider fireballs with masses $m_F \geqslant m_p$ or m_t respectively, in the corresponding directions. The function $G(\eta, \sqrt{s})$ depends in our case not only η and $\sqrt{s}$, but also on the kinematical limit and the mass of the primary particle in the direction in which the fireball is moving (compare [2, 4, 7, 8]):

$$G_{p,t}(\eta, \sqrt{s}) = Nq_0 e^{-ae^{-|\eta-\eta_{p,t}|}}\left(1-\frac{m_{p,t}\cdot 2}{\sqrt{s}}\sinh\eta\right). \tag{3}$$

The fireball temperature $T(M_F, \sqrt{s})$ depends on the incoming hadrons, especially on their masses and quantum numbers. The temperature was calculated for NN collisions as function of the energy density or mass of the fireball on the basis of the statistical bootstrap model [7–10] . For πN collisions, this was done in Ref. [4], for KN in Ref. [5]. We used the temperature functions according to the strong statistical bootstrap model as given in these papers for the corresponding cases (πN, KN, NN).

For newly produced particles, we use, in the central region, fireballs with average masses

$$M_F(\eta, \sqrt{s}) = M_0 = \text{const.} \quad \text{for} \quad |\eta| \leqslant \log\frac{\sqrt{s}}{M_0}. \tag{4}$$

With the changes discussed we obtain the formula for the newly produced particles i in collisions

$$h_p + h_t \to i(\equiv h_3) + X, \tag{5}$$

$$E\frac{d^3N_{NP_i}}{dp^3} = \int_{-\eta_t}^{\eta_p} G_{p,t}(\eta, \sqrt{s})\mu_i \cosh(\eta_i-\eta) g_i(\eta, \sqrt{s}) f_i\left(\frac{\mu_i \cosh(\eta_i-\eta)}{T_{p,t}(M_F, \sqrt{s})}\right). \tag{6}$$

The quantities with indices p and t differ in the forward and backward case. η_i is the rapidity of the considered particle i in the CMS.

(ii) Particle production by resonances of the projectile or target particles (R, Fig. 1)

The colliding particles may be excited into resonances with masses m_i^* which decay into stable hadrons. The resonances carry the additive quantum numbers of the leading primary particle. We consider only two-particle decay, where the particles i in the fireball rest frame are distributed according to the decay function [1]. The modifications discussed above are applied similarly to the resonance contribution of [1]. We assume that particles

from three and more particle decay can be approximately represented by the same decay distribution.

(*iii*) Particle production by leading resonances with changed quantum numbers (RC, Fig. 1)

In collision (5), for inclusive particle production of i, quantum number conservation determines the lowest number of particles which have to be produced in association. In Fig. 1, RC we consider the two particle decay of the leading resonances. If quantum number conservation demands three or more particles we have to consider also the associated production of the other corresponding particles. They are considered in the corresponding formulae in the same manner as in Ref. [1, 2].

The reaction

$$pp \to N^* \to \Sigma^-$$

is an example of RC, see Fig. 1, RC'. The Σ^- comes from a nucleon resonance N*, which decays to Σ^- and K^+.

π^+ is the corresponding associatively produced necessary particle.

The invariant distribution function follows in a straightforward manner in analogy to Ref. [2].

(*iv*) Through-going particles (T, Fig. 1)

This contribution has to be calculated in p or t directions, only if particle i is identical to the corresponding incoming particle. We changed the formula of Ref. [1] for collisions (5) to the invariant form with the analogous modifications discussed above.

(*v*) Through-going particles with quantum number exchange (TC, Fig. 1).

We consider a trough-going particle which changes single quantum numbers. Because of additive quantum number conservation there have to be also associatively produced

TABLE I

Used resonances and corresponding weight factors

Kind of resonance	Resonance mass m_i*[GeV]	Weight factor $a_{m_i^*} = \log_{10} A_{m_i^*}$ compare [1]	
mesons π	0.765	1.65	
	1.26	3.25 unsafe with	± 0.5
	1.66	4.65	
K*	0.89	1.8	± 0.2
	1.42	3.7	
baryons N* → (N, π)	1.236	2.05	
	1.520	2.9	± 0.1–0.2
	2.190	3.63	
N* → (Y, K)	1.670	3.33	
	2.190	4.8	± 0.2
	2.65	6.6	

additional particles. The changes in the corresponding formula of Ref. [1] which were necessary because of (5), were provided in analogy to the above contributions.

The Planck type decay function of the contribution of the new production is cut off by a phase space method [11]. The modifications of this method for h_1-h_2-collisions are described in Appendix A. The parameters used in the fireball rapidity distribution function $G_{p,t}(\eta, \sqrt{s})$ are the same as in Ref. [2]. The authors fitted the theoretical contributions of the thermodynamical model to the experimental data for pp collisions from about 5 GeV up to ISR energies. In Table I we present the weight factors of the resonances A_{m_i*} used in our calculations. Table II collects the contributions used. The weights G_i of newly pro-

TABLE II

Contributions used in the calculation of spectra

Primary particles	Considered particle	Contributions in forward direction[a]
π^- p	Λ	NP
	K^0, $\overline{K^0}$	NP, RC, TC
K^- p	π^+	NP, RC(K*)
	π^-	NP, R(K*), TC
	K^0	NP, R(K*), TC
	$\overline{K^0}$	NP
	K^-	NP, R(K*), T
	p	NP
	Λ	NP
K^+ p	K^0	NP, R(K*), TC
	$\overline{K^0}$	NP
pp	π^+	NP, R(N*), TC
	π^-	NP, RC(N*)
	K^+, K^0	NP, R(N*), TC
	K^-, $\overline{K^0}$	NP, RC(N*)
	p	NP, R(N*), T
	Λ, Σ^+	NP, R(N*), TC
	Σ^-	NP, RC(N*), TC
	$\overline{\Lambda}$	NP

[a] The contributions in the backward direction are identical to the corresponding contributions of the pp forward case.

TABLE III

Weight factors of newly produced particles

Particle	Weight factor G_i of formula (1a)
$\bar{p}$, p	1.7
$K^\pm$	0.95 } see Ref. [3]
$\pi^\pm$	1.4
K^0, $\overline{K^0}$	0.95
Λ, Σ^+, $\overline{\Lambda}$	2.0

TABLE IV

Parameters used in the thermodynamical model

Parameter	Formula/Reference	Used value
a	(3), [3]	−0.21
M_0	(4), [3]	−2.48
b	leading fireball distribution $F_0(\lambda)$ in Ref. [1, 2]	4.58

duced particles are given in Table III. The average fireball mass was taken to be $M_F = 2.5$ GeV for the calculations of newly produced particles. Table IV contains further parameters of the thermodynamical model used.

3. *Comparison with data in Kp, $\pi^{\pm}p$ and pp collisions*

In Fig. 2 we show the theoretical and experimental spectra of particles in collisions of $K^-p \to p, K^-, \overline{K^0}, \pi^{\pm}, \Lambda$. The data [13] are integrated over the transverse momenta and plotted versus $x = p^*_{\parallel}/p_{max}$ for the primary momentum of 16 GeV/c. The 32 GeV/c data

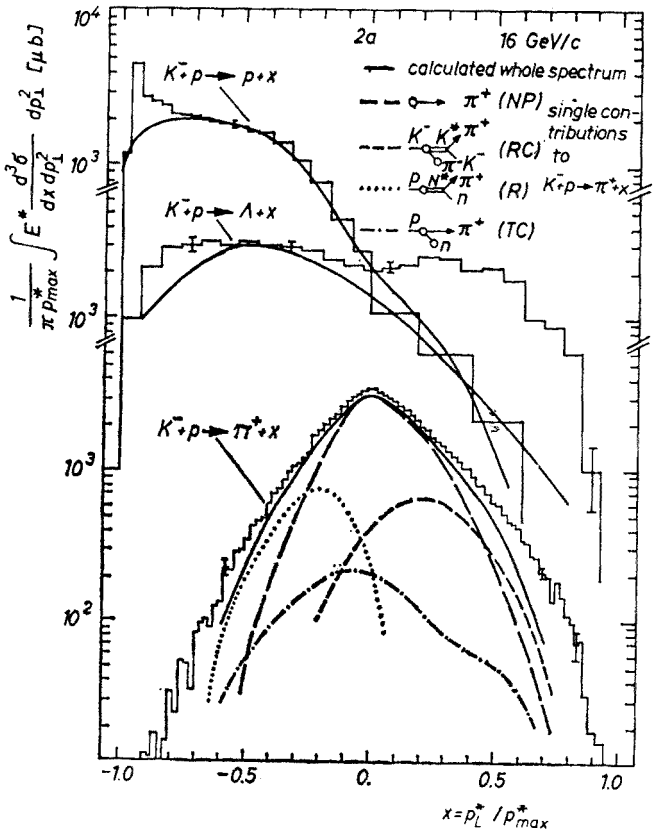

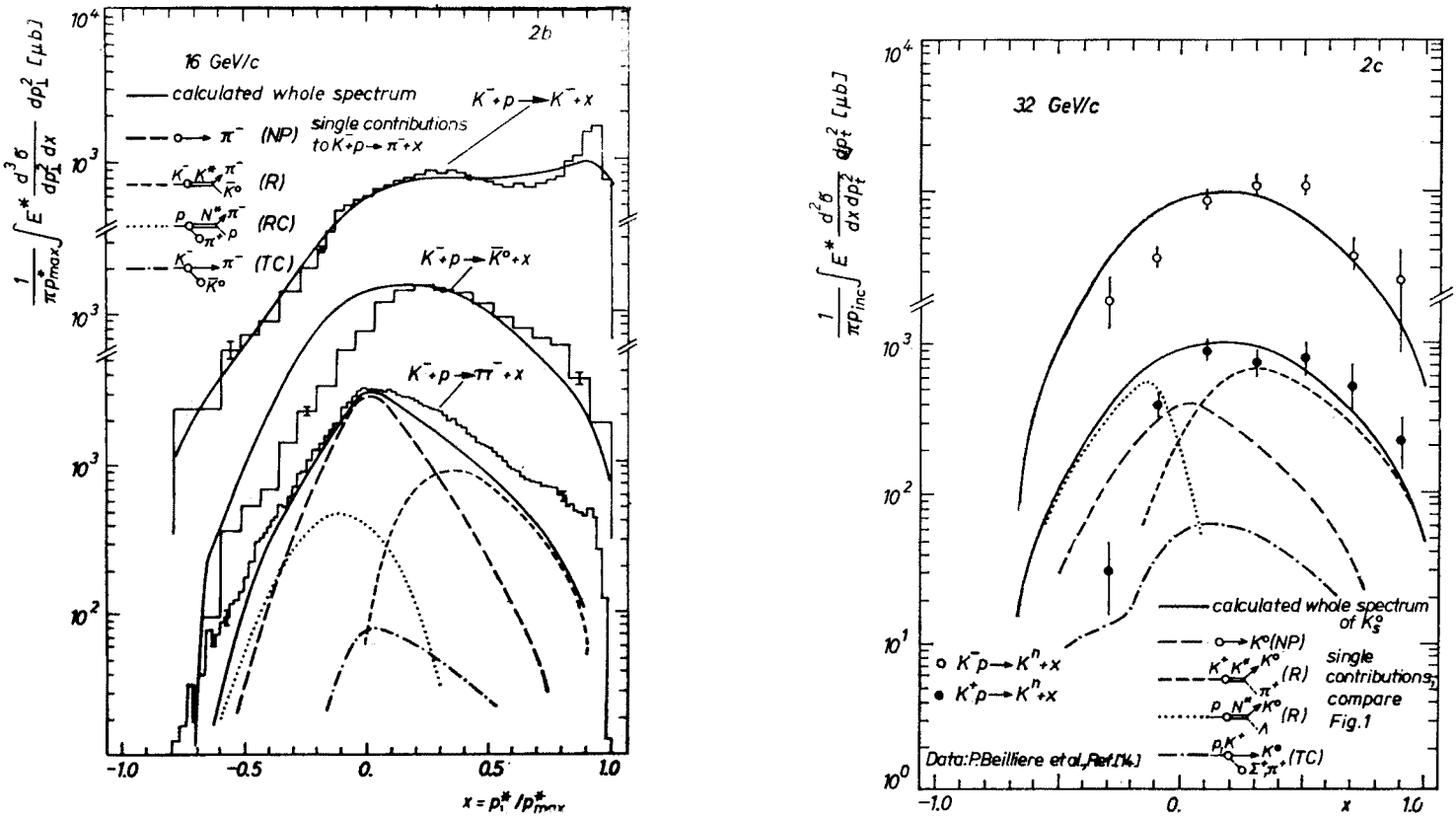

Fig. 2. K⁻p collision data in comparison with the thermodynamical model calculations at 16 GeV/c, integrated over $p_\perp^2$, plotted versus $x = p_L^*/p_{max}^*$: a — spectra of p, Λ, π^+; b — spectra of K^-, K^0, π^-; c — spectra of K^n in the collisions K^-p and K^+p. K^n means either K^0 or $\bar{K}^0$. For the reactions $K^-p \to \pi^\pm$ and $K^+p \to K^0$, we also plot the contributions considered in our calculation

were taken from Ref. [14]. We have to use new production together with resonance (RC) production for the explanation of the backward K^-, K^0 and π^- and the forward π^+ production. Resonance production of the other particles and their corresponding other directions proceeds according (R). We show also some partical contributions. The bump of the Λ-spectrum, Fig. 2a for $x > 0$, is an effect of exclusive reactions or other mechanisms like hypercharge annihilation, compare Ref. [15], within this low energy region.

In Fig. 2c for $K^{\pm}p \to K^n$ our theoretical spectra show broad maxima between $x = 0.2$ and $x = 0.3$ arising from N* and K* resonances, respectively. The forward part describes the data well. But the backward parts of the broad maxima can not be seen in the data. We determined the weight of the resonance-contributions to the whole spectrum from totally integrated differential invariant cross sections of $pp \to K^0/\bar{K}^0$ and $pp \to \Lambda$ reac-

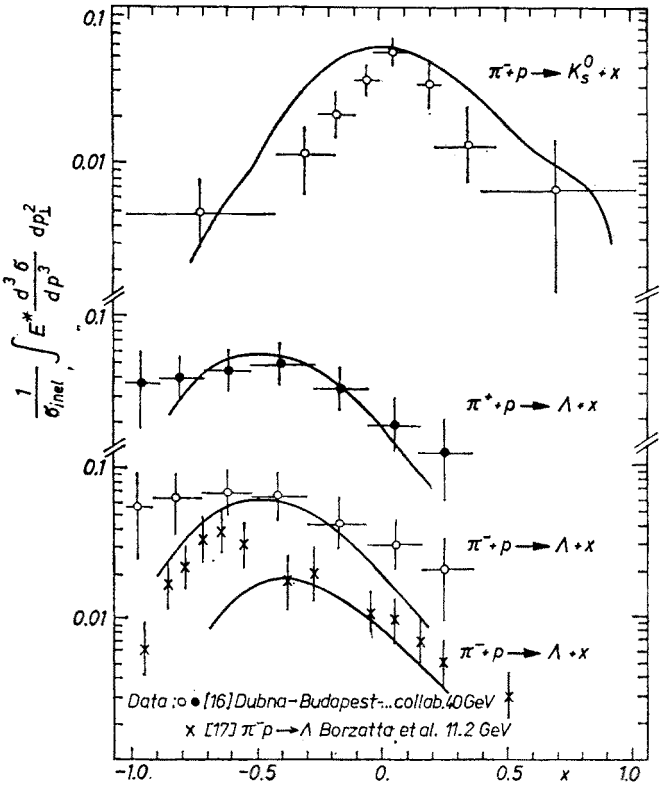

Fig. 3. Inclusive single particle spectra of Λ for $\pi^{\pm}p$ collisions and $\pi^- p \to K_s^0$ at 40 GeV/c and $\pi^- p \to \Lambda$ at 11.2 GeV/c compared with thermodynamical model calculations, integrated over $p_\perp^2$, plotted versus x

tions, to be in a good agreement with data within a broad primary momentum range. However, we use only three different weights, given in Table I, in all channels of the two particle resonance decay $N^* \to Y + K$, $N^* \to N + \pi$ and $K^* \to K + \pi$ and do not use isospin weight factors. Therefore, only limited agreement with data is possible.

We neglected the contributions of non diffractively produced resonances which would be $1/\sqrt{s}$-dependent and unimportant for higher energies. Therefore, the weight is somewhat

too high and within the low energy region appears a difference between the data and the model calculations.

For the same reason there are deviations in Fig. 2b. We summed up the K^0 and $\overline{K^0}$ contributions.

In Fig. 3 we compare Λ and K_s^0-production in $\pi^{\pm}p$ collisions at 40 GeV/c (data Ref. [16, 17]) and the 11.2 GeV/c data of Ref. [17], as a function of x integrated over $p_\perp^2$. Although the data points of the Λ distributions exhibit little difference for π^+p and π^-p collisions, we get in our model nearly identical distributions, because the main part of these Λ's comes from the leading resonances, having in both cases the same quantum numbers. The masses of the recoil particles (π^+, π^-) are equal. The influence of the kinematics creating the difference is too low. Only very small differences may be seen in the contribution of through-going particles with changed quantum numbers order 5%–10%. The energy dependence of $\pi^- + p \to \Lambda + X$ is well understood.

The production mechanisms are working for K_s^0 creation in quite another way. In this case, new production already dominates the other contributions, but resonance production is still rather strong. Therefore the shape of the corresponding curve differs obviously from that of the others in the picture.

In the central region, for $-0.2 < x < 0.0$ the calculated spectrum of the reaction $\pi^- p \to K_s^0$ is higher than in the data for the same reason discussed above for Fig. 2c. We sum up for the K_s^0 spectrum not only the K^0 contribution from backward N* resonances and the NP contribution for K^0 which are the most important contributions to K^0, but also corresponding contributions to $\overline{K^0}$.

In Fig. 4 we compare $\Sigma^{\pm}$, Λ and p spectra in pp collisions integrated over $p_\perp^2$ at 24 GeV/c as a function of $x = 2p_\parallel^*/\sqrt{s}$. We used the resonance contribution (RC) with associated particle production for the calculation of Σ^- spectra. We used, for the calculations of the other spectra the new production, the through-going contributions (T) and (TC), respectively, and the resonance contribution (R). The amounts of resonance production of Σ^+ and Σ^- are of the same order, but the differences in the data may be better explained by the essentially stronger damping in the Σ^- data than in the Σ^+ data for higher $|x|$ values (data Ref. [18]). Table II presents the thermodynamical contributions taken into account.

Fig. 5 compares $\bar{\Lambda}$ spectra for pp-collisions integrated over $p_\perp^2$ for several energies as a function of $x = 2p_\parallel^*/\sqrt{s}$ and the rapidity y_{LAB} [18, 19].

In Fig. 6 we compare Λ production data with our model in pp collisions at several energies as functions of x ([20, 21] data). The agreement in the x-distribution in Fig. 6 for $|x| < 0.5$ is rather good. The maximum values show small deviations. In the calculated curves they are too far towards higher $|x|$ values. Obviously lower-mass-resonances play a more important role than regarded up to now.

Fig. 7 gives a comparison of K^0 production in pp collisions at several energies (data [20–22]) versus x. In Fig. 8 we demonstrate the energy behaviour of the model for neutral particle production in pp-collisions [22]. We compare the behaviour of integrated distributions $\left(\int E \frac{d^3\sigma}{dp^3} \frac{dp^3}{E}\right)$ in an energy range up to 300 GeV for Λ and $K^0/\overline{K^0}$ production. The

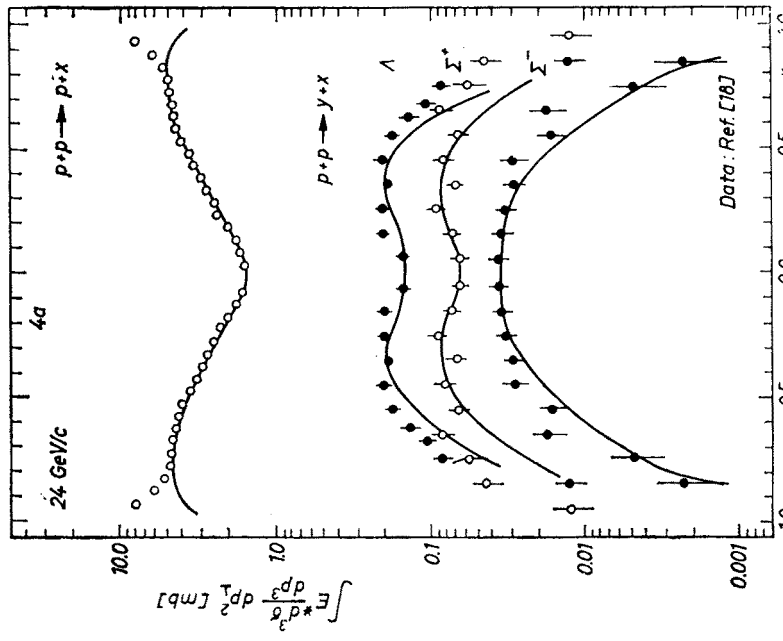

Fig. 4. Comparison of the thermodynamical model with data on p, Λ and $\Sigma^{\pm}$ in pp collisions at 24 GeV/c, integrated over $p_{\perp}^2$: a — plotted versus x; b — plotted versus y_{LAB}

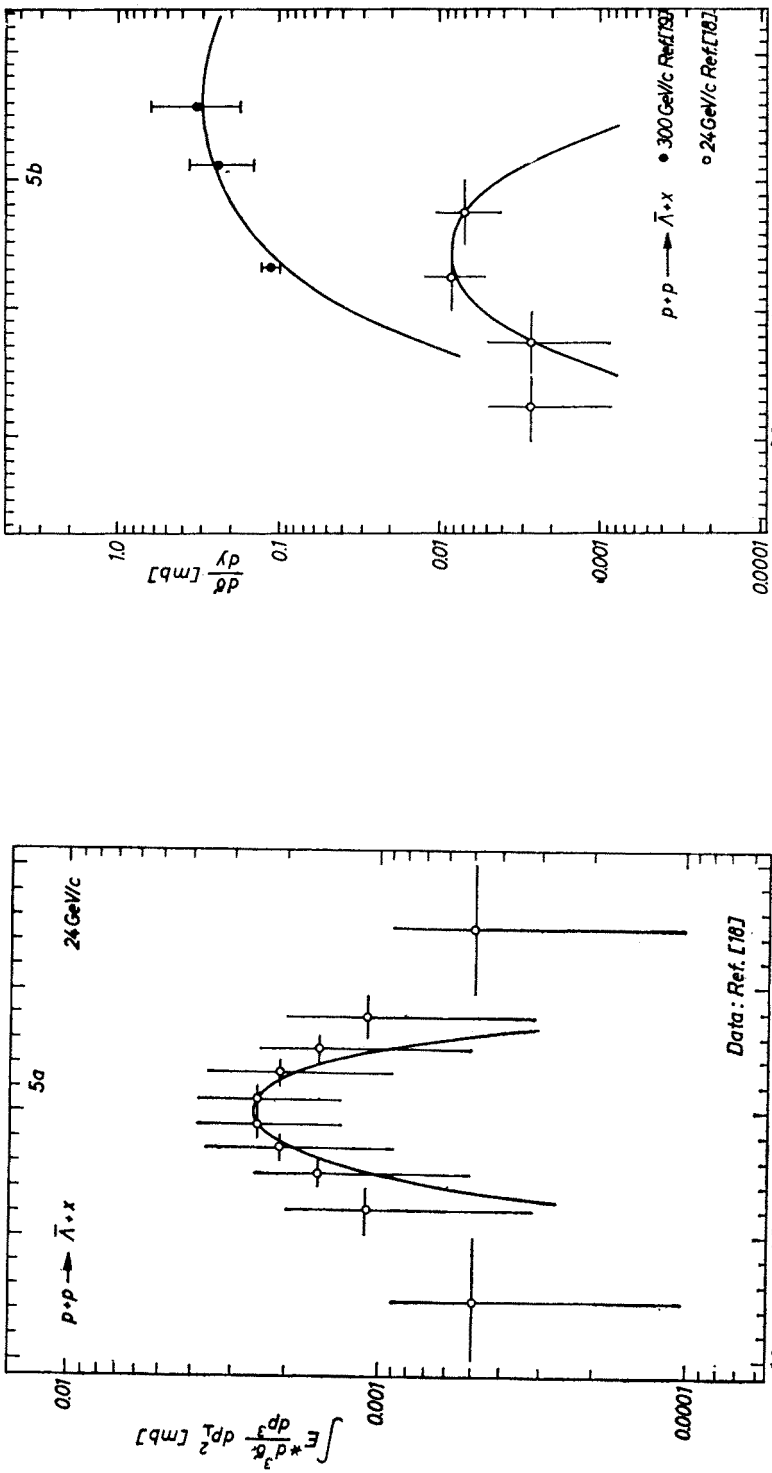

Fig. 5. $\bar{\Lambda}$ spectra in pp collisions, integrated over $p_\perp^2$ for several energies: a — plotted versus $x = 2p_\parallel^*/\sqrt{s}$; b — plotted versus y_{LAB}

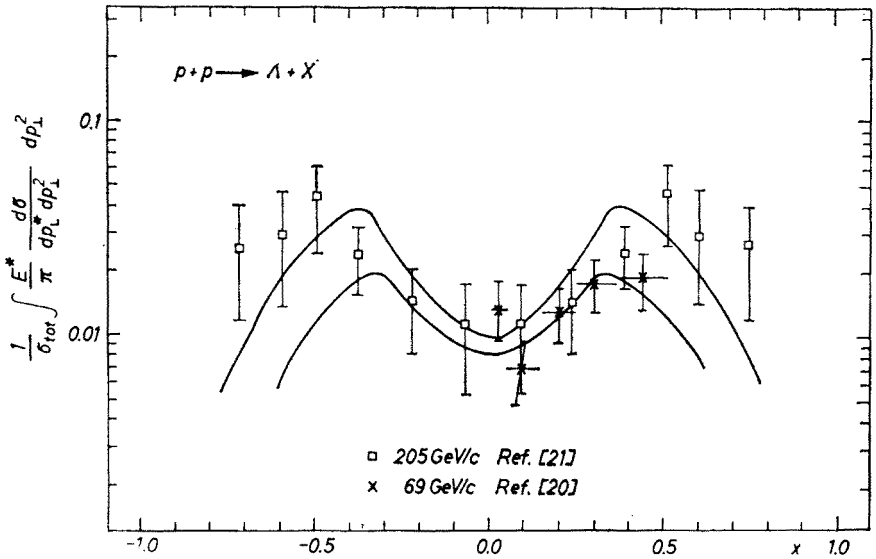

Fig. 6. Inclusive single particle spectra of Λ in pp collisions, integrated over $p_\perp^2$ compared with the thermodynamical model at several energies plotted versus x

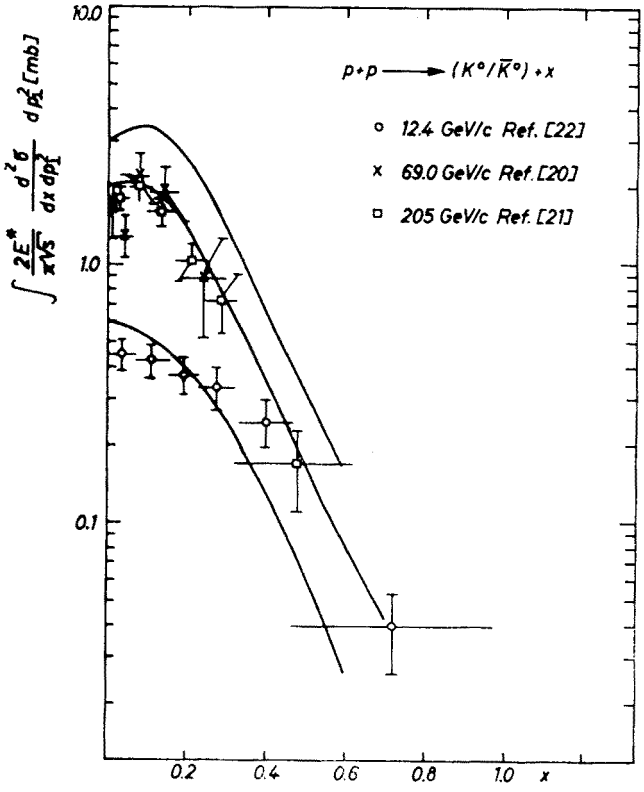

Fig. 7. Inclusive single particle distributions for $K^0/\bar{K}^0$ production in pp collisions at several engeries, integrated over $p_\perp^2$ compared with the model as function of x

model describes the $K^0/\overline{K^0}$ spectrum quite well. The model shows, however, for the Λ-spectrum for $p > 50$ GeV/c deviations. The cause is that the resonance contribution used in the model is growing too fast with energy, much more than the contribution of the new production asymptotically. This is not in agreement with current expectations of the thermodynamical model. Such a behaviour may be seen in Fig. 6 too. The calculated spectra at higher

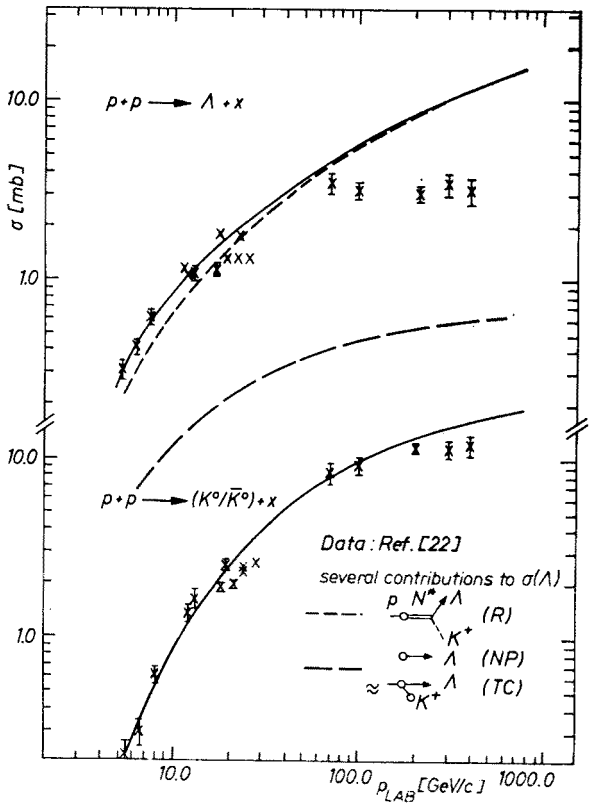

Fig. 8. Integrated single particle distributions of Λ and $K^0/\overline{K^0}$ as function of the primary momentum in pp collisions compared with the thermodynamical model, $\left(\int E \frac{d^3\sigma}{dp^3} \frac{dp^3}{E}\right)$ drawn versus p_{LAB}. In addition there are given single partial contributions

energies are not in agreement with data because of the strong increase of the resonance contribution with energy. Some small deviations from data for greater $|x|$-values ($|x| > 0.4$) are also present. The velocity distribution function of through-going fireballs, compare [1], does not have the right behaviour in the contributions (R) and (RC). These assumptions are supported by the agreement of the theoretical and experimental spectra of $\bar{\Lambda}$-production in Fig. 3.

4. Conclusion

In the central region, most of the particles (pions and kaons) are created freely, i. e., in connection with their antiparticles, at the considered energies. The production mechanism (NP) there dominates particle creation.

In the range $0.2 < |x| < 0.8$ particle production via resonances (R) becomes more important with increasing $|x|$. This production mechanism within this x-range dominates the momentum spectra if two particle decay of leading resonances is possible.

It is surprising that the model already describes the data well, although we did not use isospin weights for the different two body decay channels $K^* \to K+\pi$, $N^* \to N+\pi$ and $N^* \to Y+K$.

Resonances with changed quantum numbers (RC), see Fig. 1 (RC), provide contributions to the momentum spectra, which are not as important as contributions of resonances produced in the mechanism (R), see Fig. 1 (R), in the range $0.2 < |x| < 0.8$, compare Fig. 2a, b. But they are necessary for the explanation of the amount and slope of the momentum spectra, compare Table II and Figs. 2, 3, 4, 7, 8.

Through-going particles (T) become important in the range $0.8 < |x| \leqslant 1.0$ at the considered energies. The sharpe diffractive peak near $|x| = 1$ in reactions like $h_1+h_2 \to h_1+X$ is not described within our model.

I appreciate numerous helpful discussions with Prof. J. Ranft and his critical reading of the manuscript.

APPENDIX A

We extend the phase space cut off method [11] to collisions of hadrons of a different kind. We consider for the case of newly produced particles (Sect. 2 (*i*)) the creation via central and peripheral production, dependent on the maximum energy of this particle. We expand this method in a straight forward calculation, taking the different recoil masses into account.

In the central case, see Fig. 9a, the whole CMS energy $\sqrt{s}$ of the system is available and decays into the considered secondary particle (mass m) and several recoil particles. We assume that $m_{\mathrm{RC}_{\min}}$ is the minimal sum of masses of recoil particles produced in the central fireball. The decaying fireball (FB) in the peripheral case (mass M) has been created in the CMS. A through-going primary particle (mass m_{recoil}) is pushed into the opposite direction of this fireball according to momentum conservation, see Fig. 9b. $m_{\mathrm{RP}_{\min}}$ is the minimal sum of masses of necessary recoil particles produced in the fireball of mass M.

We obtain Lorentz-velocities

$$\gamma_{\mathrm{R}_{\mathrm{central}_{\min}}} = \frac{s-M^2-m_{\mathrm{recoil}}^2}{2Mm_{\mathrm{recoil}}}, \tag{A1a}$$

$$\gamma_{\mathrm{R}_{\mathrm{peripheral}_{\min}}} = \frac{M^2+m_{\mathrm{RP}_{\min}}^2-m^2}{2Mm_{\mathrm{RP}_{\min}}}, \tag{A1b}$$

in the fireball rest system for the minimal total mass of recoil particles in the peripheral case and in the CMS for the recoil particle in the central case, respectively. The connection of these two pictures gives the condition

$$\gamma = \gamma_{\mathrm{R}_{\mathrm{peripheral}_{\mathrm{min}}}} = \gamma_{\mathrm{R}_{\mathrm{central}_{\mathrm{min}}}}. \tag{A2}$$

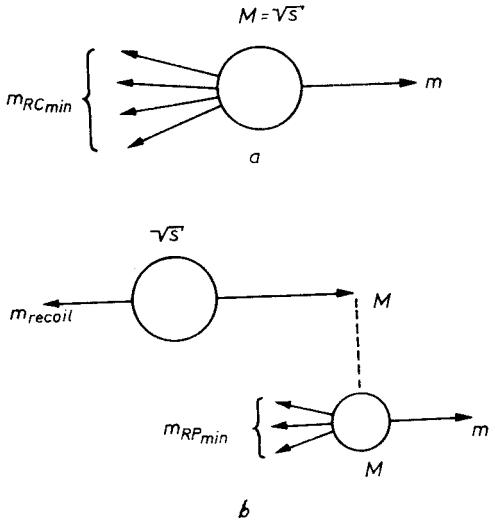

Fig. 9a. Scheme for the decay of a fireball (mass $M = \sqrt{s}$) in the central case with minimum total mass of the recoil particles. b. Scheme of a peripheral production mechanism

according to [11] and we derive

$$\bar{\gamma} = \frac{s + M^2 - m_{\mathrm{recoil}}^2}{2M\sqrt{s}} \tag{A3}$$

with

$$M^2 = \frac{m_{\mathrm{RP}_{\mathrm{min}}} s + m_{\mathrm{recoil}} m^2}{m_{\mathrm{RP}_{\mathrm{min}}} + m_{\mathrm{recoil}}} - m_{\mathrm{recoil}} m_{\mathrm{RP}_{\mathrm{min}}}. \tag{A4}$$

We choose kinematical limits in such a way that the energy of the produced secondary particle is maximal, i. e.,

$$\begin{aligned} &\text{central case for} \quad 1.0 \leqslant \gamma \leqslant \bar{\gamma}, \\ &\text{peripheral case for} \quad \bar{\gamma} < \gamma \leqslant \gamma_{\mathrm{o}_{\mathrm{p,t}}} \end{aligned} \tag{A5}$$

in the forward case is different from $\bar{\gamma}$ in the backward case.

REFERENCES

[1] R. Hagedorn, J. Ranft, *Supl. Nuovo Cimento* Vol. III, No 6, 2, 311 (1968).
[2] J. Ranft, *Phys. Lett.* **31B**, 529 (1970).
[3] J. Ranft, CERN-Lab II-RA/74 — 2 (1974).
[4] Htun Than, J. Ranft, *Nuovo Cimento Lett.* **5**, 655 (1972).
[5] E. Matthäus, J. Ranft, *Phys. Lett.* **40B**, 230 (1972).
[6] H. R. Gerhold, B. Buschbeck, *Nuovo Cimento* **22A**, 39 (1974).
[7] R. Hagedorn, J. Ranft, *Nucl. Phys.* **B48**, 157 (1972).
[8] J. Ranft, *Phys. Lett.* **41B**, 613 (1972).
[9] R. Hagedorn, *Suppl. Nuovo Cimento* Vol. III, No 2, 147 (1965); S. C. Frautschi, *Phys. Rev.* **D3**, 2821 (1971).
[10] E. M. Ilgenfritz, J. Kripfganz, *Nucl. Phys.* **B62**, 141 (1973).
[11] R. Hagedorn, J. Ranft, *Nucl. Phys.* **B48**, 191 (1972).
[12] J. Ranft, *Correlations in Multiparticle Production*, V International Symposium on Many Particle Hydrodynamics, June 4–10, 1974, Eisenach–Leipzig, p. 210; R. Kirschner, KMU-HEP — 7601 (Preprint, 1976).
[13] P. Bosetti, M. Deutschmann et al., *Nucl. Phys.* **B60**, 307 (1973).
[14] P. Beilliere, C. Cochet, J. J. Dumont et al., *Nucl. Phys.* **B90**, 20 (1975).
[15] H. Muirhead et al., *Hypercharge Annihilation*, Liverpool 1975.
[16] DBBKSTTUH Collab., *Yad. Fiz.* **T18**, 1251 (1973).
[17] P. Borzatta, L. Liotta, S. Ratti et al., *Lett. Nuovo Cimento* **7**, No. 14 (1973).
[18] V. Blobel et al., BHM Coll., DESY 73/36 (1973); *Nucl. Phys.* **B69**, 454 (1974).
[19] A. Sheng et al., CALT-68-480.
[20] H. Blumenfeld et al., *Phys. Lett.* **45B**, 525 (1973); *Phys. Lett.* **45B**, 528 (1973).
[21] G. Charlton et al., *Phys. Rev. Lett.* **30**, 574 (1973).
[22] K. Jaeger, D. Colley, L. Hyman, J. Rest, ANL/HEP 7461 (Preprint 1974).